JOURNAL OF GEOPHYSICAL RESEARCH, VOL. 106, NO. A11, PAGES 26,183–26,193, NOVEMBER 1, 2001

Sunlit Io atmospheric [O I] 6300 Å emission and the plasma torus

Ronald J. Oliversen,[1,2] Frank Scherb,[3,2] William H. Smyth,[4] Melanie E. Freed,[5,2]
R. Carey Woodward Jr.,[3,2] Max L. Marconi,[6] Kurt D. Retherford,[7,2]
Olivia L. Lupie,[8,2] and Jeffrey P. Morgenthaler[3,2]

Abstract. A large database of sunlit Io [O I] 6300 Å emission, acquired over the period 1990-1999, with extensive coverage of Io orbital phase angle ϕ and System III longitude λ_{III}, exhibits significant long-term and short-term variations in [O I] 6300 Å emission intensities. The long-term average intensity shows a clear dependence on λ_{III}, which establishes conclusively that the emission is produced by the interaction between Io's atmosphere and the plasma torus. Two prominent average intensity maxima, 70° to 90° wide, are centered at $\lambda_{III} \approx 130°$ and $\lambda_{III} \approx 295°$. A comparison of data from October 1998 with a three-dimensional plasma torus model, based upon electron impact excitation of atomic oxygen, suggests a basis for study of the torus interaction with Io's atmosphere. The observed short-term, erratic [O I] 6300 Å intensity variations fluctuate ~20-50% on a timescale of tens of minutes with less frequent fluctuations of a factor of ~2. The most likely candidate to produce these fluctuations is a time-variable energy flux of field-aligned nonthermal electrons identified recently in Galileo plasma science data. If true, the short-term [O I] intensity fluctuations may be related to variable field-aligned currents driven by inward and outward torus plasma transport and/or transient high-latitude, field-aligned potential drops. A correlation between the intensity and emission line width indicates molecular dissociation may contribute significantly to the [O I] 6300 Å emission. The nonthermal electron energy flux may produce O(^1D) by electron impact dissociation of SO_2 and SO, with the excess energy going into excitation of O and its kinetic energy. The [O I] 6300 Å emission database establishes Io as a valuable probe of the torus, responding to local conditions at Io's position.

1. Introduction

Jupiter's strong magnetic field and rapidly rotating magnetosphere and Io's volcanism combine to create dynamic physical features in the Jovian system including Io's atmosphere and plasma torus. Overlying Io's molecular atmosphere (mainly SO_2 and SO) is an extended atomic atmosphere (mainly O and S) that is dynamically shaped, electronically excited, and lost through ionization and collisionally driven escape by the impacting plasma (see review by *Spencer and Schneider* [1996]). The first atmospheric emissions detected from Io were the sodium *D* lines [*Brown*, 1974], produced by resonance scattering of sunlight, although sodium is only a trace atmospheric constituent. The plasma torus (mainly O^+, O^{++}, S^+, S^{++}, and S^{+++}) rotates with Jupiter, except very near Io's orbit, where there is a few percent corotational lag [*Brown*, 1994]. The torus results from the balance between an Iogenic heavy-ion plasma source and a radially outward plasma transport loss.

The excitation morphology of Io's atomic atmosphere is characterized by equatorial emission features ("auroral spots"), distinct limb glow, diffuse and extended emissions, and enhanced emissions on the downstream side of the plasma flow around Io, referred to as wake emissions. These features are observed for Io in eclipse by the Galileo Solid State Imaging (SSI) experiment [*Belton et al.*, 1996; *Geissler et al.*, 1999], by the Hubble Space Telescope Wide Field Planetary Camera 2 (HST/WFPC2) [O I] 6300 Å images [*Trauger et al.*, 1997], and by the HST Space Telescope Imaging Spectrograph (STIS) [O I] 6300 Å images [*Retherford et al.*, 1999; *Oliversen et al.*, 2000], and in sunlight by HST/STIS UV images [*Roesler et al.*, 1999]. The equatorial "spots", located near the sub-Jovian and anti-Jovian points, are brightest 100-200 km above Io's surface and change Iocentric latitude as Io's Jovian magnetic latitude changes, suggesting that they are associated with Birkeland currents that flow through Io or its ionosphere. The limb glow, presumably due to the presence of a diffuse global or hemispherical S and O atmosphere within several hundred kilometers of the surface, is consistently brighter on the polar hemisphere facing the plasma torus centrifugal equator. The

[1]Laboratory for Astronomy and Solar Physics, NASA Goddard Space Flight Center, Greenbelt, Maryland.
[2]Visiting Astronomer at the National Solar Observatory, Kitt Peak, Arizona.
[3]Department of Physics, University of Wisconsin, Madison, Wisconsin.
[4]Atmospheric and Environmental Research, Inc., Lexington, Massachusetts.
[5]Raytheon ITSS, Lanham, Maryland.
[6]Fresh Pond Research Institute, Cambridge, Massachusetts.
[7]Department of Physics and Astronomy, Johns Hopkins University, Baltimore, Maryland.
[8]Computer Sciences Corporation, Space Telescope Science Institute, Baltimore, Maryland.

Paper number 2000JA002507
0148-0227/01/2000JA002507$09.00

extended neutral S and O ultraviolet emissions, detected out to 10-15 R_{Io}, have an intensity profile between ~ $r^{-1.5}$ and $r^{-2.2}$ (r is distance from Io) with the brighter extended emission profile on the downstream (plasma wake) side of Io [*Wolven et al.*, 1999; B.C. Wolven et al., Emission profiles of neutral oxygen and sulfur in Io's exospheric corona, preprint, 2000].

Although these "snapshot" observations provide information on the morphology of Io's neutral atmosphere, the space-based data have sampled only a small fraction of possible Io-torus-magnetosphere configurations (e.g., orbital phase angle ϕ, System III longitude λ_{III}, System IV longitude λ_{IV}, magnetic latitude, and solar cycle). In addition, intrinsic temporal variations (e.g., due to volcanic or magnetospheric disruptions) need to be identified and distinguished from the more regular, cyclical history of Io's interaction with the plasma torus.

We report the results from a continuing, long-term, ground-based campaign of Io (not in eclipse) [O I] 6300 Å emission, covering a wide range of Io-Jovian system parameters. Observations of [O I] 6300 Å are important for understanding the Io atmosphere-plasma torus interaction since neutral oxygen is a dominant component of the atomic atmosphere; the relatively short lifetime (~130 s) of the O(^1D) state means that the emission is near its source of excitation and therefore is a diagnostic of plasma conditions. Our field of view, by including all dominant localized emission from Io's disk and exobase (~1.4 R_{Io}) and also the fainter extended emission out to 5-7 R_{Io} (the Lagrange sphere ~5.85 R_{Io}), is well suited to study the Io-plasma torus interaction. This approach is furthermore strengthened by the correlation of Io emission brightening recorded simultaneously in HST/STIS UV observations and our [O I] 6300 Å ground-based observations, as reported by *Roesler et al.* [1999]. We also present modeling of a subset of observations to illustrate the Io-plasma torus interaction and to isolate inherent, short-term time-dependent fluctuations. A comprehensive modeling analysis of the complete data set is beyond the scope of this paper and will be undertaken in future work.

2. Observations

In February 1990 we began a program of high spectral resolution ($R \approx 1.2\text{x}10^5$; $\delta\lambda \approx 0.05$ Å or $\delta v \approx 2.5$ km s^{-1}) observations of [O I] 6300 Å emission from Io's vicinity, using the stellar echelle spectrograph at the National Solar Observatory (NSO) McMath-Pierce 1.5-m telescope on Kitt Peak. Exposures are restricted to 15 min, which limits spectral smearing (< 0.1 km s^{-1}) due to Io's orbital motion. The initial wavelength scale and instrumental resolution are determined by using a thorium-argon hollow cathode lamp to illuminate the entrance aperture of the spectrograph. Calibration spectra are taken at the beginning and end of each night. The spectrograph has a Bowen-Walraven 10 slice by 200 μm image slicer at the entrance aperture with a 5.2x5.2 arcsec field of view and is coupled to a TI 800x800 charge-coupled device (CCD). Each observation is autoguided using Io's blue/green continuum (< 5800 Å) reflected from a dichroic mirror located above the entrance aperture.

This telescope and spectrograph allow the detection of narrow, relatively faint emission lines superposed on Io's

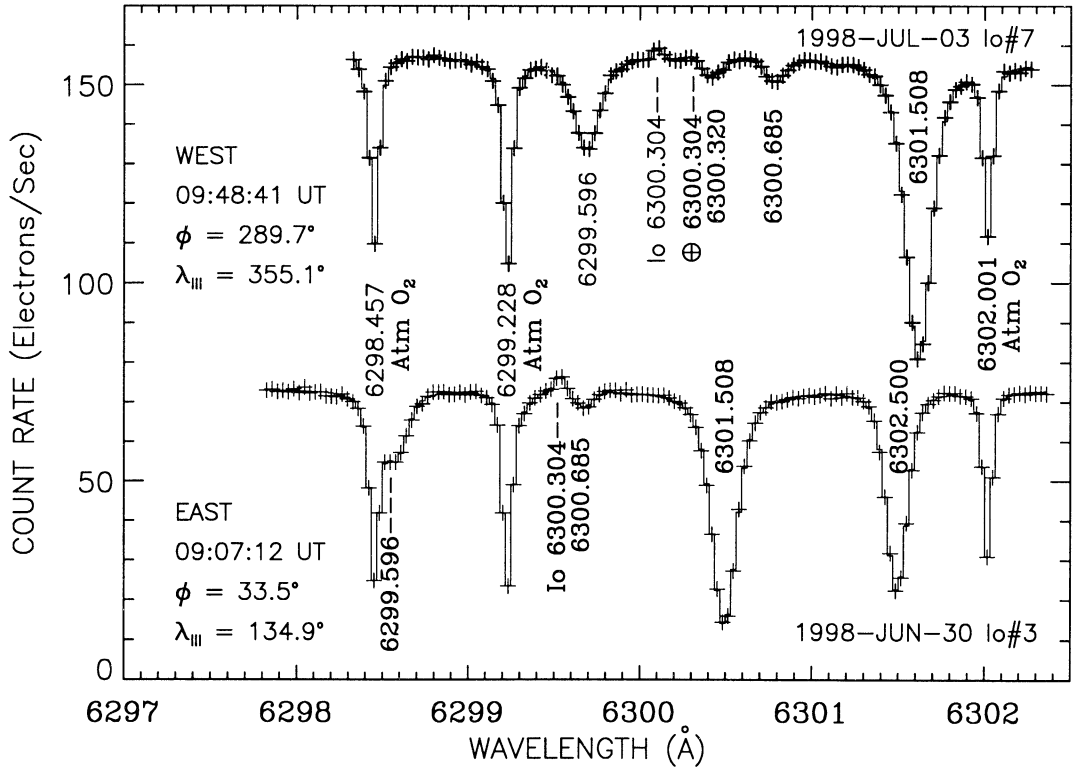

Figure 1. Examples of Io spectra. The terrestrial lines are due to O_2 absorption and [O I] 6300 Å airglow emission. The unlabeled lines are solar absorption lines. The Io [O I] 6300 Å emission is Doppler-shifted relative to terrestrial and solar lines. The bottom (top) spectrum is offset up (down) by a count rate of 25 electrons s^{-1}.

Table 1. Summary of Observations and Data Reduction

	Year								
	1990-1992	1993	1994	1995	1996	1997	1998	1999	Total
Number of nights	6	3	30	0	10	39	45	32	165
Total spectra	38	13	190	0	61	441	742	472	1957
Spectra processed	33	12	50	0	58	343	403	139	1038
Detectable [O I][a]	30	10	35	0	43	292	338	117	865
Spectra fit – west	21	0	27	0	23	184	201	63	519
Spectra fit – east	9	10	8	0	20	108	137	54	346

[a] Model successfully fit spectra with an Io [O I] 6300 Å signal-to-noise ratio > 2. The average signal-to-noise ratio is ~6.

reflected solar spectrum (Figure 1). Ten years after the first detection in 1990 [*Scherb and Smyth*, 1993], this remains the only facility that has detected sunlit Io [O I] 6300 Å emission. (*Bouchez et al.* [2000], using the Keck 10-m telescope, have recently observed [O I] 6300 Å emissions of similar intensity from Io in eclipse.) Under favorable conditions, image slicer data can be analyzed to extract some information about the spatial distribution of the emission with 0.5x0.5 arcsec spatial bins [*Potter and Morgan*, 1990]. However, because of the relative faintness of the [O I] 6300 Å signal, the data have so far been analyzed only in the total aperture-integrated mode. A summary of all data taken to date and the current state of data reductions is given in Table 1.

3. Data Analysis and Observational Results

The image slicer data are reduced with standard CCD reduction techniques, and one-dimensional spectra are extracted. The Io [O I] 6300 Å emission results are based on an iterative least squares fitting procedure. Multiple Voigt functions are used to represent solar Fraunhofer and terrestrial atmospheric absorption lines, while the Io and terrestrial atmospheric [O I] 6300 Å emission lines are represented by Gaussian functions. The fitting program can link parameters of solar or terrestrial lines together so as to minimize the number of adjustable parameters. This procedure is essential for accurate separation of the Doppler-shifted Io emission line from the underlying solar spectrum and terrestrial atmospheric absorption lines, as illustrated in Figure 1. Typically, 9 to 11 lines are included in the final fit. The earlier results reported by *Scherb and Smyth* [1993] systematically overestimated the [O I] intensity, owing to limitations in modeling the spectra, so we include their 35 spectra from the 1990-1992 data, reprocessed for consistency.

As summarized in Table 1, a total of 1038 of the observed 1957 spectra have been reduced. This includes spectra from every year since 1990 except 1995, when the McMath-Pierce telescope was closed for nighttime observations. The quality of the fits is generally quite good, with little evidence of systematic trends in the flux residuals. Using the terrestrial

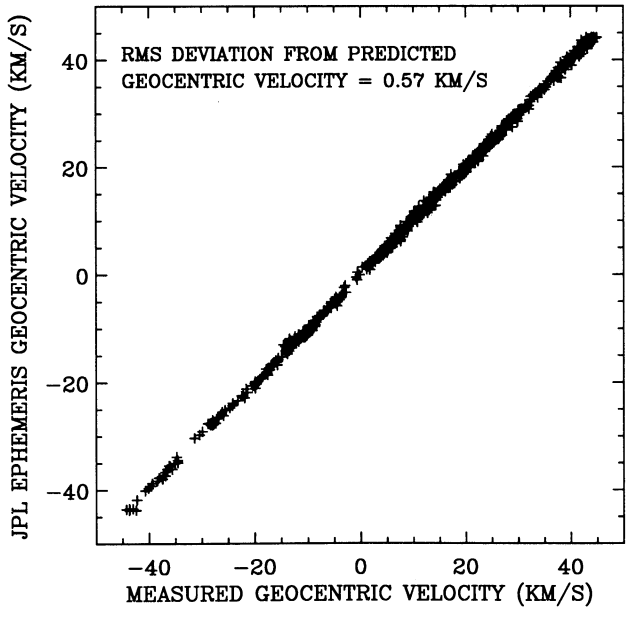

Figure 2. Correlation of measured and calculated geocentric velocity of Io [O I] 6300 Å emission. The calculated geocentric velocity is from the Jet Propulsion Laboratory (JPL) "Horizons" ephemerides program. The mean error in the Io [O I] 6300 Å line position is 0.16 km s^{-1}.

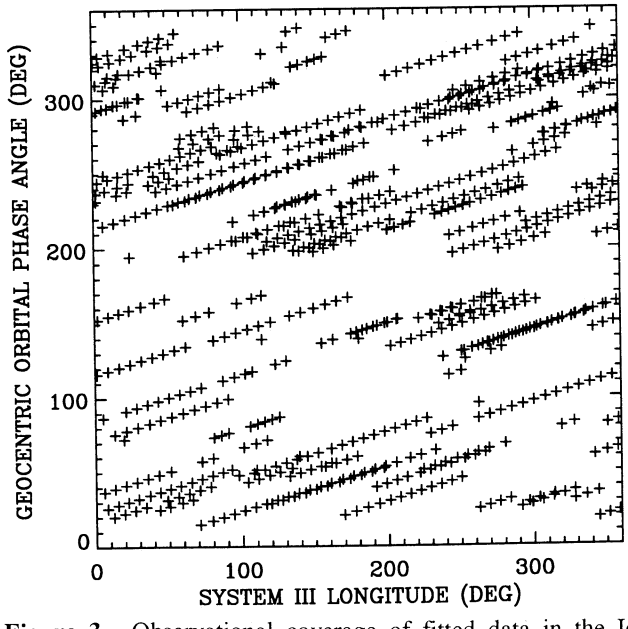

Figure 3. Observational coverage of fitted data in the Io geocentric phase angle and Io System III longitude plane. The location of each fitted spectra is denoted by a plus symbol. Observations on any single night follow a positive-sloped line pattern.

absorption lines to make a final wavelength correction (< 1 pixel) for each individual spectrum, a comparison between the predicted geocentric velocity of the Io emission line versus the fitted value gives good agreement (Figure 2). The mean difference is -0.01 km s^{-1} with a rms deviation of 0.57 km s^{-1} (0.012 Å). Despite adequate continuum signal, we are unable to fit ~17% of the spectra owing to inadequate signal-to-noise in some Io [O I] 6300 Å emission lines that were Doppler-shifted into a solar absorption feature or blended with the [O I] 6300 Å airglow. Another ~6% were fitted with the position of the Io emission feature linked to a terrestrial absorption line, but this does not appear to significantly affect the results. For the 865 fitted spectra, 60% were acquired for Io west of Jupiter and 40% were acquired for Io east of Jupiter. Our data cover much of the Io ϕ and Io λ_{III} parameter space, as shown in Figure 3. However, there are gaps, both due to observational limitations (e.g., $\phi \approx 180°$ (Io transit) or $\phi \approx 360°$ (Io occulted)) and data not yet reduced or taken (e.g., region bounded by $\phi \approx 70° - 130°$ and $\lambda_{III} \approx 130° - 240°$).

Io's reflected solar continuum is used as the intensity calibration source to correct for changes in heliocentric and geocentric distances, variations in Io's albedo as a function of orbital phase angle and solar phase angle, and changes in observing conditions. Io's surface intensity in the nearby continuum is ~4 MR/Å. Since the spatial distribution of the emission around Io is complex, an average equivalent intensity is determined by assuming that the emission is confined to Io's disk. The disk-averaged [O I] 6300 Å intensity I_{6300} varies from a lower limit (signal-to-noise > 2) of 2-3 kR up to ~20 kR. Ninety-five percent of the I_{6300} results have a signal-to-noise > 3, and the average I_{6300} signal-to-noise is ~6. These sunlit I_{6300} results are comparable to I_{6300} results obtained by HST images for Io in eclipse [*Trauger et al.*, 1997; *Oliversen et al.*, 2000], which show that the 6300 Å intensity is dominated by emission on and near Io's disk. Figure 4 shows I_{6300} as a function of λ_{III} for Io both east (dawn) and west (dusk) of Jupiter. The average value of I_{6300} is 8.1 ± 0.1 kR for Io west of Jupiter and 7.6 ± 0.1 kR for Io east of Jupiter. The factor of ~2 I_{6300} variability about its average value is real, and it is larger when Io is west of Jupiter (1σ = 3.4 kR) than when Io is east of Jupiter (1σ = 2.6 kR).

Despite the large variability in intensities evident in Figure 4, there is now enough data coverage to discern some average patterns. Averaging the [O I] intensities in 10° System III longitudinal bins shows two broad maxima ~ 70° - 90° wide, centered at $\lambda_{III} \approx 130°$ and $\lambda_{III} \approx 295°$. These broad maxima are near where Io is in the dense region of the plasma torus, crossing the plasma torus centrifugal equator (shown as dashed vertical lines in Figure 4 at λ_{III} = 112° and at λ_{III} = 292°).

Figure 5 shows the [O I] 6300 Å intensity plotted versus the convolved Full width half maximum (FWHM) line width. The plot clearly shows that, on average, line width is correlated with intensity. The details of the intrinsic emission line width are not shown in this plot; that is, we did not deconvolve the instrumental profile (FWHM typically 0.05 ± 0.005 Å). The intrinsic [O I] emission line width is not resolved for the smaller measured line widths (where it is essentially the instrumental line width) but becomes dominant for intrinsic line widths > 0.087 Å, corresponding to an approximate convolved (measured) line width of 0.1 Å.

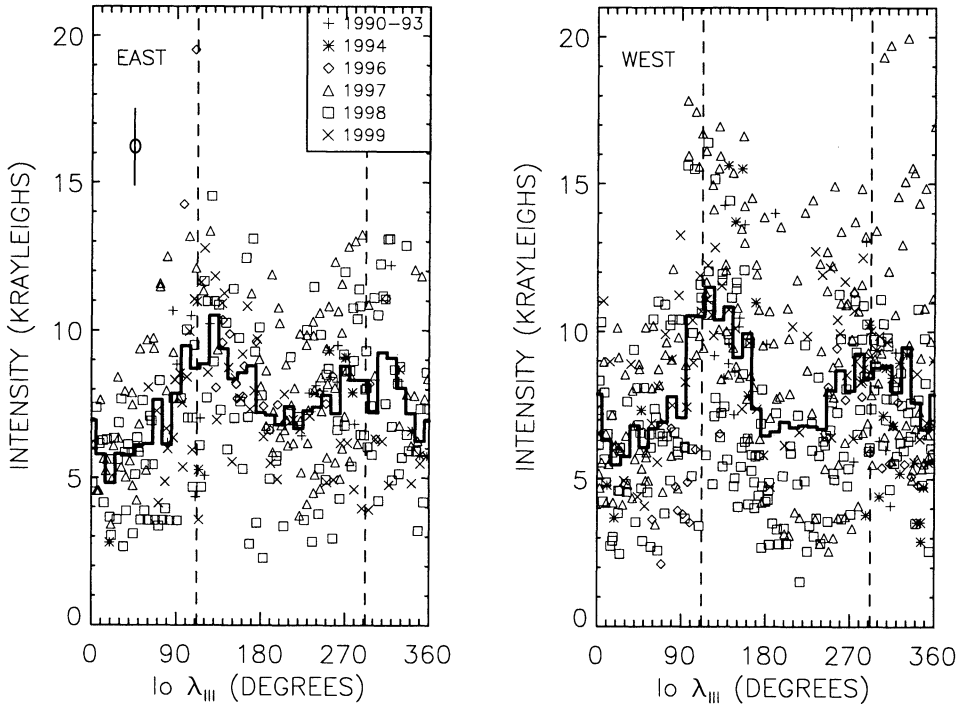

Figure 4. System III longitude behavior of the measured [O I] 6300 Å Intensity. The [O I] 6300 Å intensity is plotted on the east (left) and west (right) sides of Jupiter versus Io λ_{III}. The data are plotted with different symbols to indicate the year of observation. The mean error in intensity is 1.3 kR; a typical error bar (± 1σ) is shown in the upper left (no data at that point). The average signal-to-noise ratio is ~6. The heavy line is the average intensity within 10° longitudinal bins. Io crosses the centrifugal equator at λ_{III} = 112° and λ_{III} = 292° (dashed lines).

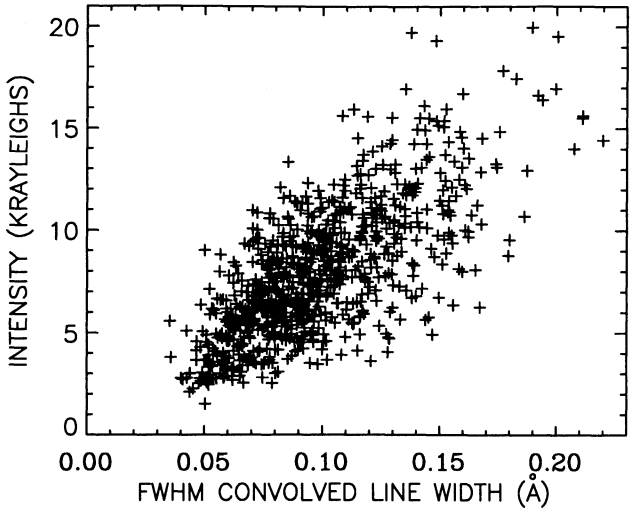

Figure 5. Correlation of the measured [O I] 6300 Å intensity and the Full width at half maximum (FWHM) convolved line width. The instrumental profile (FWHM typically 0.050 ± 0.005 Å) has not been deconvolved in the FWHM line width. The intrinsic [O I] emission line width becomes dominant for intrinsic line widths > 0.087 Å, corresponding to an approximate convolved (measured) line width of 0.1 Å.

4. Interpretation of Observations

Electron impact of atomic oxygen is a plausible excitation mechanism of the 6300 Å emissions from Io's local atmosphere, corona, and extended neutral cloud. Model emission calculations for O I 1304 Å and O I] 1356 Å from Io support the electron impact excitation of atomic oxygen [*Michael and Bhardwaj*, 2000]. Dissociative excitation of SO_2, SO, and O_2, producing $O(^1D)$ with subsequent 6300 Å emission, may also provide significant additional sources, but the importance of molecular dissociative excitation is at present uncertain. For SO_2 and SO this uncertainty arises from the lack of cross section information. Cross section information for O_2 is available, but the O_2 abundance in Io's atmosphere is expected to be too low to contribute significantly to the dayside emission [*Summers and Strobel*, 1996; *Wong and Smyth*, 2000].

Because of the lack of SO_2 and SO cross sections, in this section we consider only thermal electron impact excitation of atomic oxygen as the source for 6300 Å emissions. The emission intensity is then proportional to the line-of-sight integration of the product of oxygen density, electron density n_e, and the [O I] 6300 Å electron impact emission rate (photons cm^3 $neutral^{-1}$ $electron^{-1}$) that depends only on electron temperature T_e. (At low altitudes in Io's atmosphere, collisional quenching of $O(^1D)$ will effectively reduce the O column density available for emitting 6300 Å photons.) The spatial distributions of n_e and T_e near Io are greatly altered from conditions in the undisturbed upstream plasma torus because of the interaction of the plasma torus with Io and its atmosphere [*Saur et al.*, 1999]. However, the time for plasma to move past Io in this interaction region is likely to be measured in minutes and is therefore short compared to the time for undisturbed upstream plasma torus conditions to change significantly as Io moves about in the torus. If altered plasma properties near Io depend approximately linearly on the undisturbed upstream plasma torus conditions, then changes in the excitation source at Io can be approximately described by specifying changes in the undisturbed upstream plasma at Io's location in the torus. This assumption should be reasonable, since the emission intensity for electron impact excitation of O depends only weakly on T_e when T_e is larger than a few eV. This condition is true at Io's orbit in the undisturbed plasma torus where $T_e \approx$ 4-5 eV, and it is also generally true in the disturbed plasma very near Io where T_e is slightly smaller [*Saur et al.*, 1999]. If changes in the excitation source at Io can be specified, then changes in the effective disk-averaged O column density N_O can be determined directly from the [O I] 6300 Å data. The changes in the [O I] 6300 Å intensity then require an accurate description of the plasma torus and the radial, longitudinal, and latitudinal motions of Io in the torus.

The most detailed description of plasma torus composition and structure is based upon Voyager 1 data [*Bagenal*, 1994]. The extracted electron density profile in the centrifugal symmetry plane at the λ_{III} of the Voyager 1 encounter (near western elongation) is shown in Figure 6 in plasmacentric coordinates [see *Smyth and Combi*, 1988]. In these coordinates the overall n_e radial structure is characterized by (1) a steeply increasing n_e profile at 5 R_J with a peak at ~5.3 R_J of almost 2000 cm^{-3} (dominated by S^+); (2) an n_e trough, centered at ~5.45 R_J, with a minimum of ~850 cm^{-3}; (3) the largest n_e peak ("electron ribbon"), centered at 5.7 R_J, with over 3000 cm^{-3} (composed of a very narrow S^+ peak centered at 5.6 R_J and a broader S^{++} peak centered at 5.7 R_J); and (4) a n_e peak of ~2500 cm^{-3} located at ~5.9 R_J, followed by a gradually decreasing radial n_e profile. In addition, n_e also decreases north and south of the centrifugal equator along the magnetic field with a scale height $H \approx 1$ R_J at the electron ribbon and with H decreasing rapidly inside that radial distance.

At Io's location in the plasma torus, n_e, T_e, and consequently the I_{6300} vary significantly because of three factors: the offset dipole magnetic field, the east-west electric field, and the ~7° tilt of the plasma torus centrifugal equator

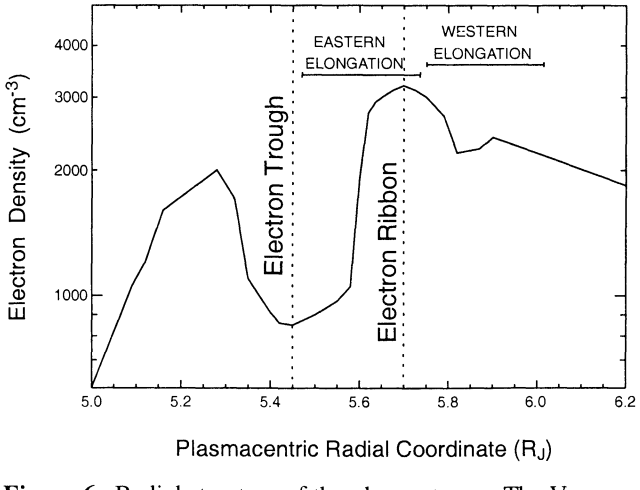

Figure 6. Radial structure of the plasma torus. The Voyager 1 n_e profile in the centrifugal equator plane of the plasma torus is shown as a function of plasmacentric radial coordinates (*Smyth and Combi*, 1988), where the electron ribbon (the maximum n_e) is always located at 5.7 R_J and the n_e trough is located at 5.45 R_J. The radial distances covered by Io at eastern and western elongation for all λ_{III} are marked.

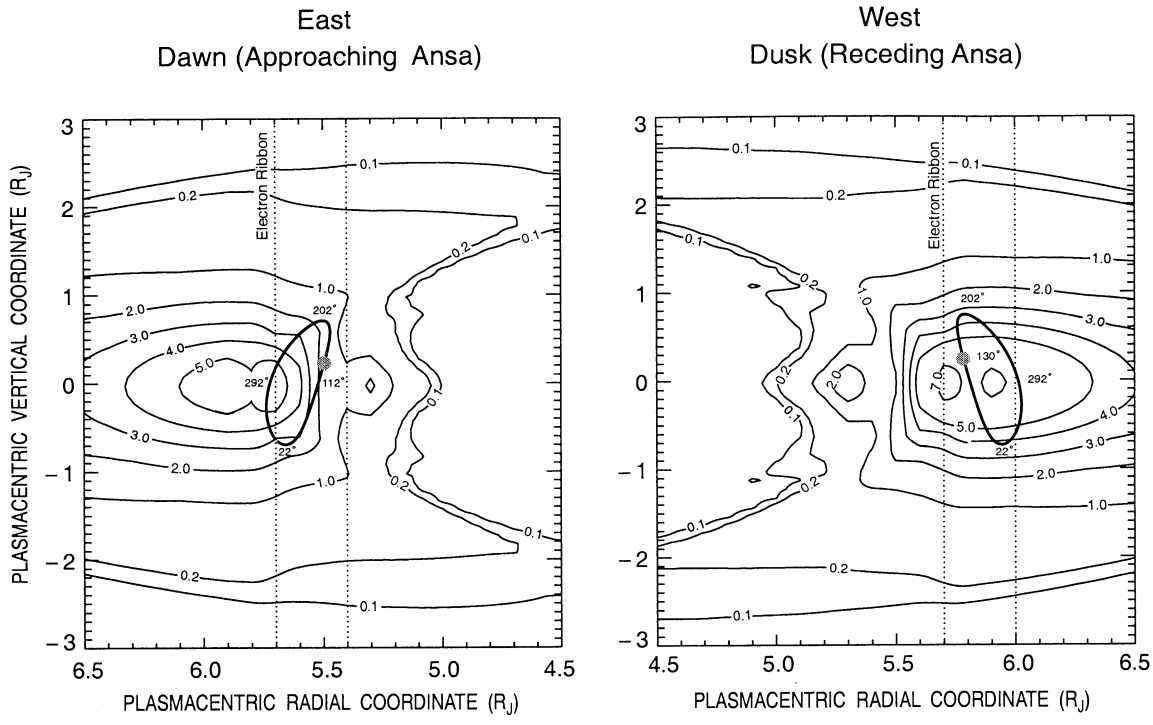

Figure 7. Two-dimensional motion of Io in the plasma torus. Io's location relative to the plasma torus electron ribbon (bold line) is shown in the plasmacentric coordinates at eastern elongation (dawn or approaching ansa) on the left and at western elongation (dusk or receding ansa) on the right. Io (shaded circle) moves around the tilted oval as a function of λ_{III} as indicated by the four angles. [O I] 6300 Å intensity contours (in kilorayleighs) in the torus, based upon electron impact excitation for undisturbed plasma conditions and $N_O = 1 \times 10^{15}$ cm^{-2}, are shown for Io (dot on oval) at $\lambda_{III} = 130°$.

plane relative to Io's orbital plane. The offset distance is 0.131 R_J from the center of Jupiter toward $\lambda_{III} \approx 149°$ for the O_4 magnetic field dipole approximation adopted here. This λ_{III} offset motion at western elongation is primarily responsible [*Smyth and Marconi*, 1998] for the ±0.073 R_J variation about the S^+ ribbon mean location of 5.57 R_J [*Schneider and Trauger*, 1995] and the ±0.165 R_J variation about the S^{++} ribbon mean location of 5.59 R_J [*Dessler and Sandel*, 1992]. The east-west electric field [*Barbosa and Kivelson*, 1983] causes the magnetospheric plasma to travel approximately on a circle with the center nominally displaced ~0.15 R_J toward eastern elongation at Io's orbit. The ~7° tilt toward $\lambda_{III} = 202°$ of the plasma torus centrifugal equator plane relative to Io's orbital plane causes Io's latitude to range north and south by ~0.75 R_J. These three factors combine to produce significant radial and vertical motions of Io relative to the structure of the plasma torus.

For Io at eastern (dawn ansa) and western (dusk ansa) elongations the radial plasmacentric range of motion of Io relative to the radial structure of the plasma torus is illustrated in Figure 6. At western elongation, Io is always outside the electron ribbon peak, while at eastern elongation, Io traverses the low n_e trough region and the electron ribbon. Io's locus in both radial and vertical plasmacentric coordinates is illustrated at eastern and western elongations in Figure 7, where Io is confined to an oval [see *Smyth and Combi*, 1988]. Io moves around the oval in a counterclockwise direction at eastern elongation and in a clockwise direction at western elongation, as indicated by the increasing λ_{III}. Also shown in Figure 7, for Io located at $\lambda_{III} = 130°$ (shaded circle on the oval), are contours of the [O I] 6300 Å emission intensity (kilorayleighs) produced by electron impact excitation. The calculation is based upon the undisturbed plasma conditions in the torus and a disk-averaged oxygen column N_O of 1 x 10^{15} cm^{-2}. The plasma torus model adopted [*Smyth and Combi*, 1988] is based upon Voyager 1 plasma properties near western elongation for an offset-tilted dipole magnetic field model and a nominal ratio of east-west electric field to corotational electric field of 0.025. In addition, the functional dependence of the λ_{III} asymmetry in the "active sector" [*Hill et al.*, 1982], based upon measurements by *Morgan* [1985a, 1985b], is included. For model-data comparisons we chose an asymmetry factor that enhances the electron density and hence the [O I] 6300 Å emission intensity by a factor of 2 in the "active sector". The electron impact rate adopted for [O I] 6300 Å emission is from *Smyth and Marconi* [2000].

At western elongation the maximum I_{6300} does not occur when Io is in the centrifugal equator at $\lambda_{III} \approx 112°$ (zero vertical coordinate, radial coordinate ~5.8 R_J). The maximum I_{6300} is located near $\lambda_{III} \approx 130°$ when Io is north of the centrifugal equator but radially closest to the electron ribbon center (see Figure 7). When Io is farthest north ($\lambda_{III} \approx 202°$) of the centrifugal equator, the proximity of Io to the electron ribbon also slightly enhances the I_{6300} minimum. I_{6300} then increases as Io moves back toward the centrifugal equator at $\lambda_{III} \approx 292°$, and I_{6300} is there further enhanced by the λ_{III} asymmetry in this angular region (the "active sector"). A minimum I_{6300} occurs near $\lambda_{III} \approx 22°$ when Io is farthest south

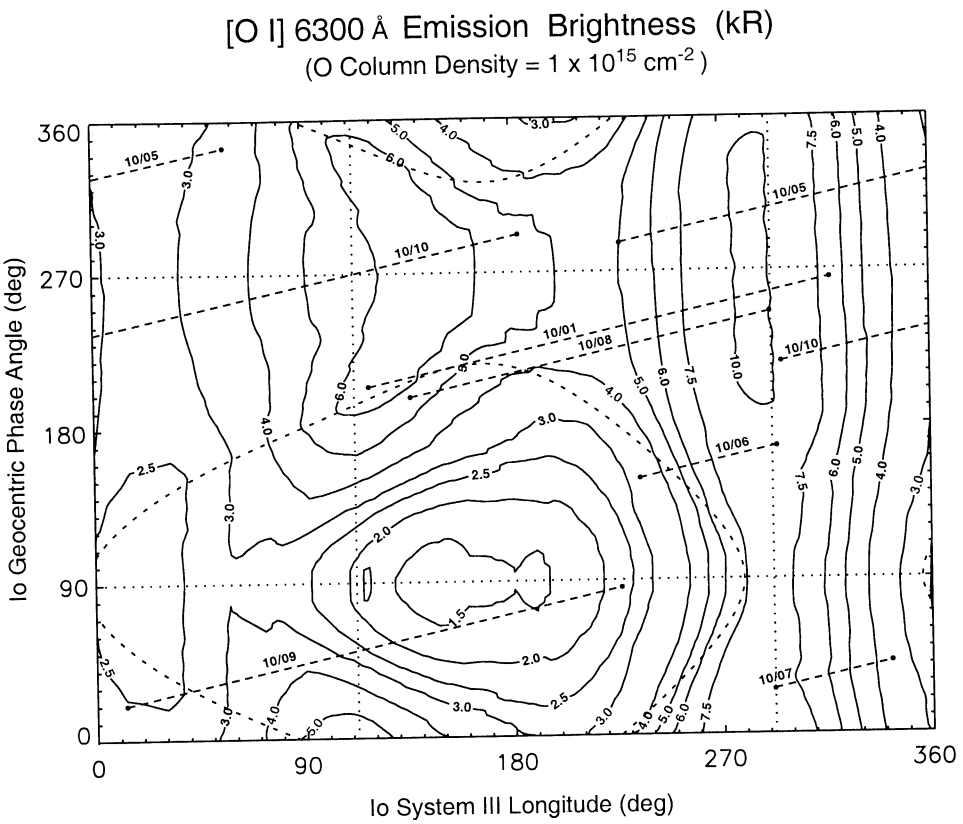

Figure 8. Model [O I] 6300 Å emission intensity at Io's location in the plasma torus. A contour plot of the [O I] 6300 Å intensity (in kilorayleighs) is shown as a function of Io ϕ and λ_{III} for N_O = 1 x 10^{15} cm^{-2}. Horizontal dotted lines are at ϕ = 90° (eastern elongation) and ϕ = 270° (western elongation). Vertical dotted lines are at λ_{III} = 112° and λ_{III} = 292°, where Io's orbital plane and the plasma torus centrifugal equator plane intersect. The dashed sloping lines are Io's paths during ground-based observations on each of 7 nights in 1998. The large dashed oval centered on eastern elongation indicates Io's angular location when it is the radial distance of the electron ribbon (5.7 R_J). Io is radially inside (outside) the peak of the electron ribbon peak for angular regions inside (outside) the dashed oval.

of the centrifugal equator and also farthest removed from the electron ribbon. At eastern elongation the maximum I_{6300} does not occur when Io is in the centrifugal equator at $\lambda_{III} \approx$ 112° since Io is radially removed from the electron ribbon and rapidly falling into the n_e trough (see Figure 6). The maximum I_{6300} occurs near $\lambda_{III} \approx$ 70° because of proximity to the electron ribbon while minimum I_{6300} occurs at $\lambda_{III} \approx$ 170° when Io is deepest in the n_e trough. For local times between eastern and western elongation the density is symmetric about each elongation point for a purely east-west directed electric field as assumed here.

I_{6300}, based upon undisturbed plasma conditions and a disk-averaged oxygen column N_O of 1 x 10^{15} cm^{-2}, is shown in Figure 8 as a function of ϕ and λ_{III} and is based upon the same plasma torus model adopted in Figure 7. The large dashed asymmetric oval centered on eastern elongation (ϕ = 90°) indicates Io's angular location when it has the same plasmacentric radial distance as the center of the electron ribbon at 5.7 R_J but may have any allowable plasmacentric vertical distance. Io is therefore radially inside of the electron ribbon peak for regions inside the dashed asymmetric oval including the n_e trough, and Io is radially outside of the electron ribbon peak for regions outside of the dashed oval including Io at western elongation (see Figure 6). For Io west of Jupiter the signature of the electron ribbon density enhancement is seen in Figure 8 as the large boomerang-shaped intensity area with an inner contour of 6 kR, organized at $\lambda_{III} \approx$ 130°. This intensity maximum provides the model basis for the observed peak at $\lambda_{III} \approx$ 130° in the ground-based I_{6300} data for Io west of Jupiter. In Figure 8, another intensity maximum occurs at $\lambda_{III} \approx$ 285° - 290° for all Io geocentric phase angles, very near where Io crosses the centrifugal equator, and is further elevated by the "active sector" enhancement included in the plasma torus model. For Io east of Jupiter the n_e trough produces the large intensity minimum symmetrically organized about eastern elongation and centered at $\lambda_{III} \approx$ 165°. Preceding this minimum, there is a predicted broad local saddle-point maximum at eastern elongati on centered near $\lambda_{III} \approx$ 70°. The averaged intensities for Io east of Jupiter (integrating the intensity in Figure 8 from ϕ = 0° to ϕ = 180°) and west of Jupiter (integrating the intensity in Figure 8 from ϕ = 180° to ϕ = 360°) are shown in Figure 9. These average intensity profiles peak near λ_{III} = 130° and λ_{III} = 290° for Io west of Jupiter and near λ_{III} = 90° and λ_{III} = 290° for Io east of Jupiter.

It is not surprising, given the variability of the [O I] intensities, that the data are not adequately represented by a static model based on Voyager 1 data and a fixed λ_{III}

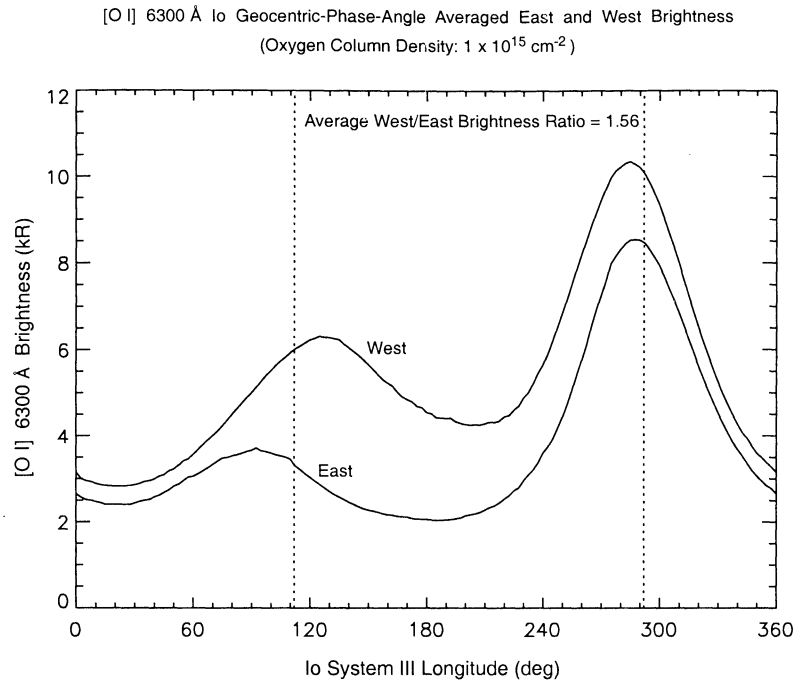

Figure 9. System III longitude model behavior for the averaged [O I] 6300 Å intensity for Io east and west of Jupiter.

dependence for emission enhancement in the active sector. The model predicts an overall average west to east intensity ratio of 1.56 when integrating the intensity profiles over λ_{III}, in comparison to the average observed west to east intensity ratio of 1.07 ± 0.01. The larger model ratio is due to the factor of 2 enhancement in the "active sector" and the lower intensity maximum on the east side at $\lambda_{III} \approx 90°$, followed by the n_e trough ($\lambda_{III} \approx 110°$ to $\lambda_{III} \approx 240°$). As noted earlier (see Figure 3), the paucity of data in the n_e trough region tends to lower the observed intensity ratio. Another difference between the model and observed average intensity profiles is that the peak at $\lambda_{III} \approx 130°$ is larger than the peak at $\lambda_{III} \approx 295°$ (Figure 4) while the model predicts the opposite. This difference is due to the enhancement in the "active sector" that is constant in the model but is clearly variable and often smaller in the data. Although these discrepancies are not completely understood and indicate the necessity for time-dependent parameters, the model is still a useful tool for describing the Io-torus interaction under certain favorable conditions.

To illustrate this, we have chosen data from seven nights (October 1 and 5-10) in 1998 to compare to the model. The angular intervals covered by these observations are shown in Figure 8 by dashed sloped lines. Comparisons of observed intensity (x in a square, with error bars) and calculated intensity (open circle) are shown in Figures 10 (Io west of Jupiter) and 11 (Io east of Jupiter) as a function of λ_{III}. The calculated intensity profiles provide a qualitative consistency (except in Figure 11c) to the observations for $N_O = 9 \times 10^{14}$ cm^{-2}. However, there are several noteworthy deviations. For example, the October 10 observations (Figure 10a) indicate the possibility of higher n_e near the $\lambda_{III} \approx 295°$ maximum with increasing latitude (see Figure 7) as the observed intensities are systematically higher than the model calculation. There are examples of intensity changes not explained by this model, implying time variability in plasma torus properties. For example, there are short-term fluctuations on the timescale of tens of minutes where the [O I] emission brightens significantly (e.g., Figure 10a, $\lambda_{III} = 0°$ to $\lambda_{III} = 10°$; Figure 10d, $\lambda_{III} = 276°$ to $\lambda_{III} = 286°$) or decreases significantly (e.g., Figure 10d, $\lambda_{III} = 260°$ to $\lambda_{III} = 290°$). There are, moreover, other deviations on a larger scale. In Figures 10c and 10d the observations sampled very similar paths in Figure 8 between the electron ribbon and the n_e trough. Although the observed intensity profiles between $\lambda_{III} = 110°$ and $\lambda_{III} = 200°$ are very similar in shape, the intensity profiles between $\lambda_{III} = 200°$ and $\lambda_{III} = 270°$ are dramatically different. For Io east of Jupiter the model provides an overall good fit for the observed intensities on October 6 (Figure 11a) and October 7 (Figure 11b), but the model was not able to fit the data on October 9 (Figure 11c) without adjusting N_O. Even then, while a reasonable fit is made for the data between $\lambda_{III} = 0°$ and $\lambda_{III} = 90°$ for $N_O = 1.5 \times 10^{15}$ cm^{-2}, the model predictions are too low owing to the effects of the n_e trough between $\lambda_{III} = 110°$ and $\lambda_{III} = 230°$. Alternatively, the model needs to be adjusted, and n_e needs to be increased in Figure 11c; otherwise, N_O has to change by ~67% on the timescale of 24 hours both before and after October 9.

5. Discussion

The model comparison (Figures 10 and 11) is a first attempt to describe the basic character of the observed λ_{III} profiles with $N_O = 9 \times 10^{14}$ cm^{-2} (except possibly for Figure 11c) over a short 7-night time interval. The general agreement, although not complete, suggests a physical understanding for study of the plasma torus interaction with Io's atmosphere for the 10 years of data. This approach provides a basis to (1) identify large-scale temporal changes in the spatial structure of the plasma torus (e.g., changes in the electron ribbon location with local time and longitudinal asymmetries in λ_{III} and λ_{IV}), (2) quantify the size and

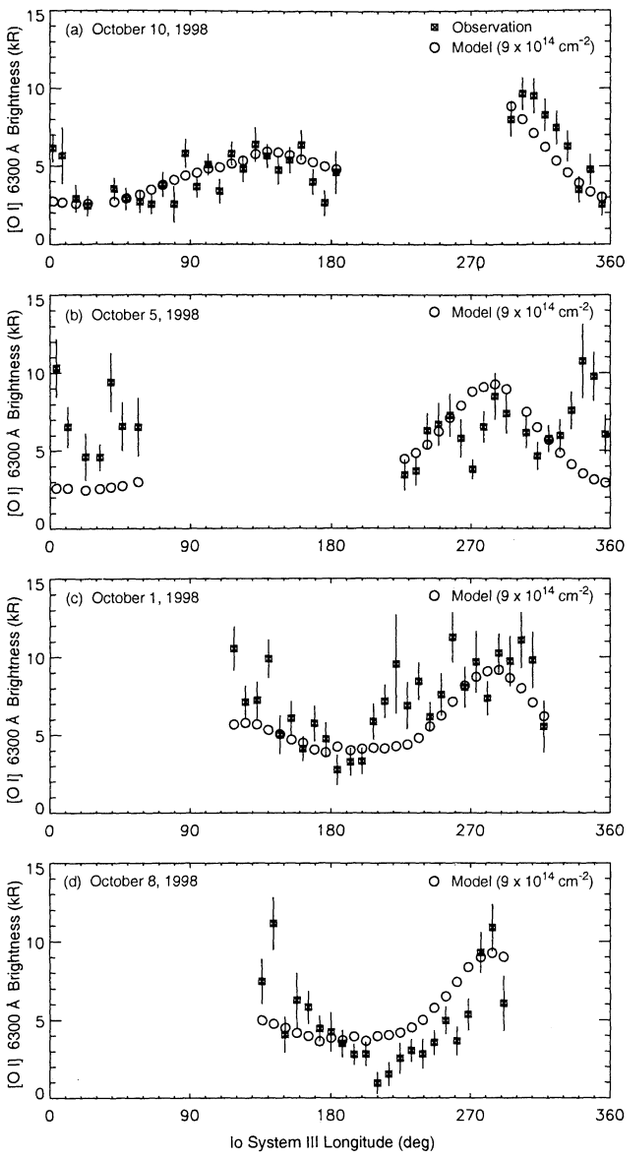

Figure 10. (a-d) Comparison of observed and model intensities for Io west of Jupiter. The observed intensity (x in a square, with error bars) and the calculated intensity (open circle) are compared as a function of Io λ_{III}. The calculated intensity is based on $N_O = 9 \times 10^{14}$ cm^{-2}.

frequency of significant intensity fluctuations and study their origin, and (3) untangle changes that occur in plasma torus n_e and in Io's atmospheric N_O. The modeling of Io's interaction with the plasma torus [Saur et al., 1999], radio occultation measurements of Io's ionosphere and wake [Hinson et al., 1998], and recent Galileo plasma wave data for the I25 close flyby of Io's south pole [Gurnett et al., 1999] suggest that n_e in much of Io's atmosphere is expected to be enhanced by an order of magnitude or more from the undisturbed upstream conditions, and the upstream $T_e \approx 5$ eV is expected to become smaller with decreasing altitude near Io. For electron impact excitation of atomic oxygen, the value $N_O = 9 \times 10^{14}$ cm^{-2} determined for undisturbed upstream conditions is then reduced by an order of magnitude or more and hence roughly requires in Io's atmosphere a line-of-sight unquenched N_O of ~9×10^{13} cm^{-2} or less. Since recent model estimates for N_O in Io's dayside atmosphere [*Wong and Smyth*, 2000] are generally larger than 1×10^{15} cm^{-2}, less than ~10% of the oxygen column would be unquenched to produce the observed intensity.

The 10-year data set in Figure 4 indicates that the base plasma model used in Figures 10 and 11 should also be adjusted on longer timescales. Although the model predicts brighter [O I] emission at the $\lambda_{III} \approx 290°$ maximum compared to the $\lambda_{III} \approx 130°$ maximum, Figure 4 shows the opposite behavior. Thus the large model "active sector" asymmetry is not dominant for a majority of the Io orbits sampled.

The detectable frequency of point-to-point fluctuations in the observed intensity profiles is limited by the ~20 min sampling time for successive data points. These fluctuations in intensity (typically ~20-50%) and larger departures (typically a factor ~2) are a general property of the data set, as illustrated in Figures 4, 10, and 11. Three possible causes of the fluctuations and larger departures are (1) time variability in Io's unquenched atomic oxygen column density, (2) spatial gradients in the plasma torus, and (3) time dependence in the field-aligned plasma torus electron flux. For the first possibility, time variability for significant changes in atmospheric column densities is measured in hours [*Wong and Smyth*, 2000] and is hence too slow to account for the

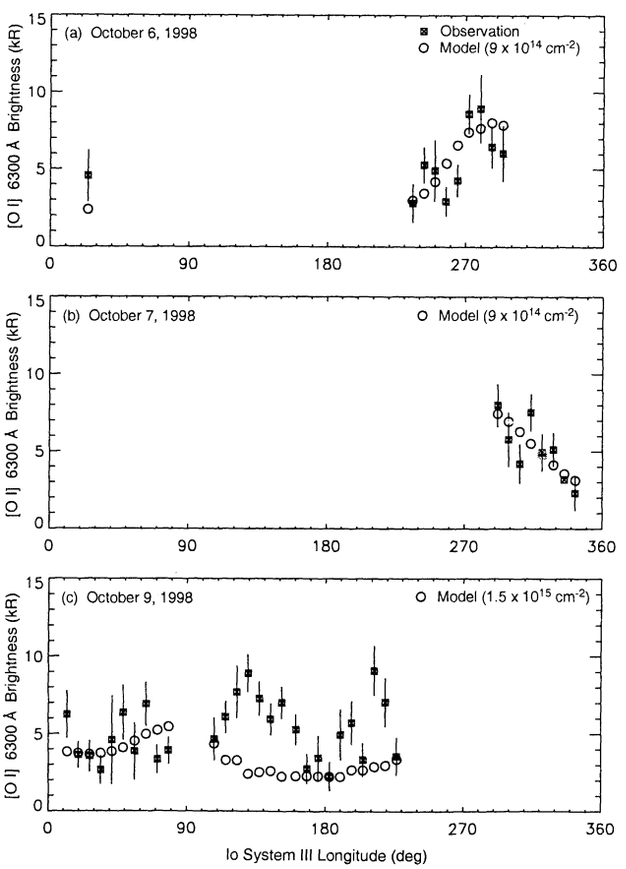

Figure 11. (a-c) Comparison of observed and model intensities for Io east of Jupiter. The observed intensity (x in a square, with error bars) and the calculated intensity (open circle) are compared as a function of Io λ_{III}. The calculated intensity is based on $N_O = 9 \times 10^{14}$ cm^{-2} for October 6 and 7, 1998, with a larger value of $N_O = 1.5 \times 10^{15}$ cm^{-2} adopted for October 9, 1998.

point-to-point fluctuations. The constancy of N_O for six of the seven profiles in Figures 10 and 11 implies that the larger departures are also not caused by atmospheric column changes. For the second possibility, significant fluctuations between two successive data points would imply longitudinal gradients with a spatial scale of ~1 R_J, which is unlikely throughout the plasma torus, whereas larger departures could possibly be due to longitudinally asymmetric torus structures. The third possibility, fluctuations of the field-aligned electron flux, is the most likely candidate, since significant fluctuations in the intensity of neutral O and S ultraviolet emissions near Io on timescales of a few to 10 min have been observed with HST [*Ballester et al.*, 1997]. Nearly instantaneous changes in the emission intensity at Io can be produced by impact of a time-dependent, field-aligned flux of electrons with energies from a few eV to more than 100 eV.

Significant fluctuations in the plasma torus field-aligned electron flux were recently documented in the December 7, 1995, Galileo - Io encounter data for electron energies >100 eV [*Frank and Paterson*, 2000]. For energies from 0 to ~200 eV a preliminary analysis of the Galileo data (W.R. Paterson, personal communication, 2000) shows that the electron distribution is reasonably well fitted by a relatively stable thermal (~4-5 eV) core population and a small, fluctuating, primarily field-aligned nonthermal (~30-40 eV) tail population. Although the total (thermal plus nonthermal) electron flux changes only several percent, the total electron energy flux fluctuates by 30 to 50% on timescales of order 10 min or less with an erratic frequency pattern. There are also less frequent factor of ~2 or more variations on timescales of several tens of minutes. Since the electron energy flux is the appropriate physical parameter for electron impact excitation in Io's atmosphere, where the electrons are all collisionally consumed, it provides an explanation for the short-term fluctuations in the [O I] 6300 Å emission. These fluctuations in the electron energy flux may explain other observed changes in Io's emissions, such as on October 14, 1997, when both O and S ultraviolet emissions and I_{6300} brighten simultaneously [*Roesler et al.*, 1999]. The I_{6300} fluctuation timescales may measure the spatial scales or timescales of the field-aligned electron energy flux and may be related to a combination of the scale sizes of the inward and outward plasma transport cells or the transient nature of high magnetic latitude field-aligned potential drops.

The Galileo electron distribution also provides an explanation for the short-term temporal variability or time-dependent "flashes and sparkles" of the 685 Å intensity of the torus S^{++} plasma ribbon observed in the Voyager ultraviolet spectrometer (UVS) data [*Sandel and Broadfoot*, 1982; *Volwerk*, 1997]. The electron impact emission rate for the S^{++} 685 Å (18-eV photons) emission is extremely sensitive to the high-energy tail of the electron distribution. For the ~4 to 5 eV component the emission rate is a factor of ~1/50 of that for the fluctuating ~30 eV component, but there are ~100 times more thermal than nonthermal electrons. Hence the stable and fluctuating electron contributions to the S^{++} 685 Å intensity are competitive. This extreme ultraviolet S^{++} intensity variability is in contrast to the observed short-time stability of the optical S^+ emission lines (6716 Å and 6731 Å) in the plasma torus, which are insensitive to T_e so the fluctuating electron contribution is too small to be significant. The "flashes and sparkles" of the 685 Å intensity of the torus S^{++} plasma ribbon are not limited to Io's vicinity, which supports the idea that the spatial inhomogeneity of the fluctuating electron component is a volumetric and natural phenomenon that occurs throughout the plasma torus.

Although the model focuses on an atomic oxygen source for the [O I] 6300 Å emissions, molecular dissociative excitation may also be a significant contributor. The nonthermal electron energy flux fluctuations provide a rationale for the correlation of I_{6300} and its measured Doppler width, shown in Figure 5, since this flux can modulate the production rate and kinetic energy of exothermic $O(^1D)$ created by electron impact molecular dissociation of SO_2 and SO. For example, an exothermic energy of 1.33 eV, corresponding to oxygen with velocity of 4 km s^{-1}, would give a total Doppler width of 0.17 Å. To further investigate this possibility, however, the important cross sections for SO_2 and SO need to be pursued in laboratory studies.

6. Summary

These [O I] 6300 Å observations demonstrate that Io is a unique, valuable probe of the plasma torus, responding to local conditions at Io's position. Thus, by observing Io's emissions remotely, we sample the small-scale, three-dimensional structure of the torus, which is not possible with remote torus emission observations that necessarily provide data integrated along the line of sight. These observations characterize the average properties of the Io-torus interaction, but the data show significant long- and short-term variations. We suggest that the short-term variation may be explained by changes in the torus electron energy flux. In addition, we present evidence for significant SO_2 and/or SO contributions to the [O I] 6300 Å emission. In the interpretation of the observational results, we utilized a particular model of the torus, based on Voyager 1 and ground-based measurements. It is clear that this static model does not account for some of the complex, time-dependent behavior of the Io-torus interaction, but that it does describe the interaction under certain favorable conditions and provides a context to understand the short-term variations.

We plan more comprehensive studies of the existing [O I] 6300 Å database including additional reductions and more observations to help characterize Io's atmosphere, torus mean global properties, and time-dependent departures from the mean. The study will help probe possible connections between time-dependent phenomena and the time-variable, nonthermal electron energy flux in the plasma torus, and the scale size of the plasma transport cells and/or field-aligned potential drops. Further observations of Io [O I] 6300 Å emission will help to fill in undersampled regions of the two-angle domain in Figure 8, especially when done in conjunction with other observational programs. Studies of the Io [O I] 6300 Å database and other Jovian-related databases provide a powerful tool to advance our understanding of interactions in the Io-torus-Jupiter system.

Acknowledgments. Given the magnitude of this program, it would not have been possible without the assistance of many people. We gratefully acknowledge the observing assistance of Patricia Chow, Nathaniel Doane, Edward Mierkiewicz, George Hilton, and Andrew Steffl; the data reduction assistance of Jason Corliss; discussions with Fred Roesler; and the support of the late Jurgen Rahe. We thank the NSO staff, especially Trudy Tilleman for her assistance with the observations and spectrograph maintenance. NSO is operated by the Association of Universities for Research in Astronomy, under cooperative agreement with the National Science

Foundation. We thank the referees for their comments. This research was supported by the NASA Planetary Research Program under RTOP 344-32-30 to GSFC and grants NAGW-3319 and NAG5-6787 to the University of Wisconsin-Madison, STIS contract NAS5-30131 to the University of Wisconsin, and by the NASA Planetary Atmospheres Program under contract NASW-96020 to AER, Inc.

Janet G. Luhmann thanks Andrew E. Potter and another referee for their assistance in evaluating this paper.

References

Bagenal, F., Empirical model of the plasma torus: Voyager measurements, *J. Geophys. Res. 99*, 11,043-11,062, 1994.

Ballester, G.E., J.T. Clarke, M. Combi, D.F. Strobel, N. Larsen, M.A. McGrath, M. Lenigan, J. Ajello, N.M. Schneider, and D. Rego, Io's far-ultraviolet emission as observed with HST and IUE (abstract), *Bull. Am. Astron. Soc., 29*, 980, 1997.

Barbosa, D.D., and M.G. Kivelson, Dawn-dusk electric field asymmetry of the Io plasma torus, *Geophys. Res. Lett., 10*, 210-213, 1983.

Belton, M.J.S., et al., Galileo's first images of Jupiter and the Galilean satellites, *Science*, 274, 377-385, 1996.

Bouchez, A.H., M.E. Brown, and N.M. Schneider, Eclipse spectroscopy of Io's atmosphere, *Icarus, 148*, 316-319, 2000.

Brown, M.E., Observation of mass loading in the Io plasma torus, *Geophys. Res. Lett. 21*, 847-850. 1994.

Brown, R.A., Optical line emission from Io, *In Exploration of the Planetary System*, edited A. Woszczyk and C. Iwaniszewska, pp. 527-531, D. Reidel, Norwell, Mass., 1974.

Dessler, A.J., and B.R. Sandel, System III variations in apparent distance of the plasma torus from Jupiter, *Geophys. Res. Lett., 19*, 2099-2103, 1992.

Frank, L.A., and W.R. Paterson, Observations of plasmas in the Io torus with the Galileo spacecraft, *J. Geophys. Res., 105*, 16,017-16,034, 2000.

Geissler, P.E., A.S. McEwen, W. Ip, M.J.S. Belton, T.V. Johnson, W.H. Smyth, and A.P. Ingersoll, Galileo imaging of atmospheric emissions from Io, *Science, 285*, 870-874, 1999.

Gurnett, D.A., W.S. Kurth, A. Roux, and S.J. Bolton, Plasma wave observations during the Galileo flybys of Io (abstract), *Eos Trans. AGU, 80* (46), Fall Meet. Suppl., F638, 1999.

Hill, T.W., M.F. Thomson, and C.K. Goertz, Some consequences of corotating magnetospheric convection, *J. Geophys. Res., 87*, 8311-8314, 1982.

Hinson, D.P., A.J. Kliore, F.M. Flasar, J.D. Twicken, P.J. Schinder, and R.G. Herrera, Galileo radio occultation measurements of Io's ionosphere and plasma wake, *J. Geophys. Res.*, 103, 29,343-29,357, 1998.

Michael, M. and A. Bhardwaj, FUV emissions on Io: Role of Galileo-observed field-aligned energetic electrons, *Geophys. Res. Lett., 27*, 3137-3140, 2000.

Morgan, J.S., Temporal and spatial variations in the Io torus, *Icarus, 62*, 389-414, 1985a.

Morgan, J.S., Models of the Io torus, *Icarus, 63*, 243-265, 1985b.

Oliversen, R.J., et al., HST/STIS visible sodium and oxygen images of Io in eclipse (abstract), *Eos Trans. AGU, 81* (19), Spring Meet. Suppl., P32A-04, 2000.

Potter, A.E., and T.H. Morgan, Evidence for magnetospheric effects on the sodium atmosphere of Mercury, *Science, 284*, 835-838, 1990.

Retherford, K.D., et al., HST-Galileo Io campaign: Images of sodium and oxygen emissions in eclipse (abstract), *Eos Trans. AGU, 80* (46), Fall Meet. Suppl., F612, 1999.

Roesler, F.L., H.W. Moos, R.J. Oliversen, R.C. Woodward, K.D. Retherford, F. Scherb, M. McGrath, W.H. Smyth, P.D. Feldman, and D.F. Strobel, Far ultraviolet imaging spectroscopy of Io's atmosphere with HST/STIS, *Science, 283*, 353-357, 1999.

Sandel, B.R., and A.L. Broadfoot, Io's hot plasma torus - A synoptic view from Voyager, *J. Geophys. Res., 87*, 212-218,1982.

Saur, J., F.M. Neubauer, D.F. Strobel, and M.E. Summers, Three-dimensional plasma simulations of Io's interaction with the Io plasma torus: Asymmetric plasma flow, *J. Geophys. Res., 104*, 25,105-25,126, 1999.

Scherb, F. and W.H. Smyth, Variability of [O I] 6300-Å emission near Io,. *J Geophys. Res., 98*, 18,729-18,736, 1993.

Schneider, N.M. and J.T. Trauger, The structure of the Io torus, *Astrophys. J., 450*, 450-462, 1995.

Smyth, W.H., and M.R. Combi, A general model for Io's neutral gas cloud. II. Application to the sodium cloud, *Astrophys. J., 328*, 888-918, 1988.

Smyth, W.H., and M.L. Marconi, An explanation for the east-west asymmetry of the Io plasma torus, *J. Geophys. Res., 103*, 9091-9100, 1998.

Smyth, W.H., and M.L. Marconi, Io's oxygen source: Determination from ground-based observations and implications for the plasma torus, *J. Geophys. Res., 105*, 7783-7792, 2000.

Spencer, J.R., and N.M. Schneider, Io on the eve of the Galileo mission, *Ann. Rev. Earth Planet. Sci., 24*, 125-190, 1996.

Summers, M.E., and D.F. Strobel, Photochemistry and vertical transport in Io's atmosphere and ionosphere, *Icarus, 120*, 290-316, 1996.

Trauger, J.T., K.R. Stapelfeldt, G.E. Ballester, J.T. Clarke, and WFPC2 Science Team, HST observations of [O I] emission from Io in eclipse (abstract), *Bull. Am. Astron. Soc., 29*, 1002, 1997.

Volwerk, M., System III and IV modulation of the Io phase effect in the plasma torus, *J. Geophys. Res., 102*, 24,403-24,410, 1997.

Wolven, B.C., H.W. Moos, P.D. Feldman, K.D. Retherford, D.F. Strobel, W.H. Smyth, F.L. Roesler, and R.J. Oliversen, Emission profiles of neutral oxygen and sulfur in Io's exospheric corona (abstract), *Bull. Am. Astron. Soc., 31*, 1166, 1999.

Wong, M.C., and W.H. Smyth, Model calculations for Io's atmosphere at eastern and western elongations, *Icarus, 146*, 60-74, 2000.

M.E. Freed, and R.J. Oliversen, Code 681, NASA Goddard Space Flight Center, Greenbelt, MD 20771. (freed@stis.gsfc.nasa.gov; ron@midnight.gsfc.nasa.gov)

O.L. Lupie, Computer Sciences Corporation, Space Telescope Science Institute, Baltimore, MD 21218.

M.L. Marconi, Fresh Pond Research Institute, 64 Fairfield Street, Cambridge, MA 02410. (marconi@freshpond.org)

J.P. Morgenthaler, F. Scherb, R.C. Woodward Jr., Department of Physics, University of Wisconsin, Madison, WI 53706. (jpmorgen@wisp.physics.wisc.edu, scherb@wisp.physics.wisc.edu; woodward@wisp.physics.wisc.edu)

K.D. Retherford, Department of Physics and Astronomy, Johns Hopkins University, Baltimore, MD 21218.

W.H. Smyth, Atmospheric and Environmental Research, Inc. 131 Hartwell Avenue, Lexington, MA 02421. (wsmyth@aer.com)

(Received September 14, 2000; revised December 5, 2000; accepted December 5, 2000.)